Prediction and Attenuation of Ground Vibrations Generated by Moving Trains

Shamsul Bashir[1, 3, b], Aamir Rashid Chowdhary[* 2, 3, b] and Nasim Akhtar[3, c]

[1,2]Academy of Scientific and Innovative Research (AcSIR), Ghaziabad-201002, India

[3]CSIR-Central Road Research Institute, New Delhi-110025, India.

[*]Corresponding author, Email: shamsulbashir123@gmail.com

[b] Ph. D Research Scholar

Email: aamirrashid606@gmail.com

[c] Sr. Principal Scientist

Email: crri.nasim@gmail.com

Abstract

The vibration generated by underground trains and the level of vibration attenuated along the propagation path are the keys to designing mitigation measures to avoid adverse effects on the surroundings. The attenuation of vibrational energy due to geometrical and material damping was determined at Civil Court Godown, Pune Metro, India, up to 30 m. The seismic cross-hole test was used to determine the dynamic properties of the soil. It was found that the soil stratum was homogeneous and composed of basaltic rock. The total vibration level reaching the receiver was predicted for trains traveling at 80, 250, and 350 km/h, and vibration attenuation measures such as steel-mass spring systems (S-MSS) and polyurethane MSS (P-MSS) were proposed.

Keywords: seismic velocity, vibration attenuation, mitigation measures, S-MSS, P-MSS

Introduction

Vibration through the soil caused by different sources can be a nuisance to humans, affecting human health conditions and having severe consequences for structures falling above it. The moving trains generate forces within the ground strata that propagate as ground-borne vibrations (GBV). For underground lines, the vibration energy transfers from the track to the tunnel wall, thereby exciting the adjacent soil medium and propagating to the surface, where it travels as surface waves. GBV can take multiple paths from the vibration source to the receiver end. These

vibrations will propagate through the ground as different waveforms, such as surface waves (R and L waves) with an elliptical particle motion in a vertical plane (R-67%), shear waves (S-waves) with particle motion perpendicular to the direction of propagation (26%), and compression waves (P-waves) with particle motion in the direction of propagation (7%)[1,2]. The P and S waves spread with hemispherical wave-fronts through the soil stratum, with their damping properties being inversely proportional to the distance from the source. R-wave travels along the ground with a circular wave-front having a damping property that is inversely proportional to the square root of the distance. Yang and Hsu (2006)[3] reported that adopting the wave numbers appropriate for the study of loads moving within the ground for the functions of spreading waves remains a significant problem and must be considered. The properties of these waves, mainly the speed of waves, are impacted by the soil stratum's characteristics, particularly the stratum's stiffness and denseness, along with the groundwater table[4]. Soil transfers track vibrations to spread an area, which is more probable to resonate with structures since the natural frequencies of most buildings are placed below 10 Hz[5-7]. The vibrations radiating into buildings significantly rely on the soil-structure interaction[5, 7, 8]. Therefore, the vibrations traveling through soil should be carefully studied for a particular location, as should the trend of wave propagation and the soil and volumetric decay of vibrations.

Throughout subway operation, the vibration energy incessantly reduces from the source to the receiver[9]. Finally, the amount of vibration that reaches the surface is 62% of the vibration generated at the source[10]. Furthermore, ground surface vibrations (GSV) of a tunnel built in stiffer soil are often considerably lower[11], and the impact of soil depth significantly depends on the excitation frequency and natural frequency of the soil strata. Based on the source's primary vibration frequency spectrum and the soil strata's transmission attributes, GSV bounces locations

vary for different vibration sources and soil stratum conditions[12]. Eitzenberger[13] investigated that when the vibration energy travels from the soil to the substructure, this energy is reflected at the interface because of dynamic impedances between the two mediums, which end up in a reduction of the vibration level[14, 15]. Zou et al.[16] found that the interaction between the soil and the structure significantly affects the vibration transmission from the ground to the building. Typically, for a multi-storey ferroconcrete building with a basement on a foundation at an overall depth of 4 to 5 m, a significant reduction in the vibration level between the bottom surface and the building is established for a comparatively thick layer of softer material overlaying the rock. For foundations in contact with the rock, coupling loss is often thought to be zero[17]. At intervals of 0–200 Hz frequency domain, the attenuation index is attenuated with the rise of underground structure stiffness.

The vibration increases as the speed of the train increases. Yao and Fang[18] investigated whether factors such as the speed of the train, the distance between the track and the building, the density of the soil, and the soil's damping can significantly impact the vibrations generated by a train. Also, if the speed of the train overpasses the R-waves within the soil stratum, a ground vibration boom happens, with a massive enhancement of the vibration energy induced. With the increase in train speed, the critical speeds are invariably more significant than the Rayleigh wave speed, whether or not the soil is hard or soft, and softer soils end up at the lower overall critical speed of the system[19, 20].

Therefore, before designing a mitigation measure to control these vibrations for a particular railway line, the vibration decay characteristics of the soil along that location should be known, and the possible consequences of ground vibration should also be considered[21, 22]. The main objective of this research is to predict the attenuation of vibrational energy generated by moving

trains due to geometrical and material damping. For trains traveling at 80, 250, and 350 km/h, the total vibration level reaching the receiver was anticipated, and vibration attenuation mechanisms such as S-MSS and P-MSS were suggested.

Ground vibration propagation and attenuation

Until now, various studies have been conducted on the decay characteristics of the vibration propagating through the soil, and geometric and material damping are the two major contributors that attenuate the vibration from the source to the receiver end[23].

Geometric Damping

In geometric damping, the energy density of the vibrational motion (body wave) decreases as the distance (x) increases because of the increasing wavefront of the sphere-shaped body wave and hence the area of wave propagation[24]. Also, energy density decays by a factor of x^2 because the sphere surface increases with the square of the distance, and the total wave energy remains constant. The radiation damping of body waves is proportional to x since the energy density (e) is directly proportional to the square of the vibration amplitude $i.e., e\ \alpha\ A^2$. Also, Attewell and Farmer[25] found that the amplitude of body waves attenuates with x. Now, in the case of the surface waves, the energy spreads in a cylindrical wavefront, not a spherical wavefront. The amplitude of these waves decays proportionally with $\sqrt{x}$ [25-27]. Woods[28] formulated the geometric damping relations with the propagating wave and the source in terms of amplitude (A) and deduced that for the attenuation of body waves in the near field and far field, the amplitude is inversely proportional to $x^2$and x, respectively. For the attenuation of surface waves, the amplitude is inversely proportional to $\sqrt{x}$. According to Athanasopoulos et al. (2000)[29], geometric damping is generally expressed in Equation (1).

$$A_s(VdB) = A_0\left({}^{x}/_{x_0}\right)^n \quad (1)$$

Where $A_s(VdB)$ is the vibration amplitude at a distance x from the source, A_0 is the amplitude at a distance of x_0 from the source, and n is the coefficient of geometric attenuation. The value of n depends on the type of source, the location of the source, and the type of wave. Tables 1 and 2 present the values of the coefficient of geometric attenuation formulated by different authors.

Gotowski and Dym[26] described the geometric decay of a wave in terms of the source-dependent parameter (S). The values of the S for different sources are given in Table 1. Equation (2) is the governing equation for calculating vibration attenuation using the S.

$$A_s(VdB) = \mathrm{S}\log\frac{x}{x_0} \quad (2)$$

Material Damping

Material damping is caused by the loss of friction between the material particles and some other form of energy. This loss is the internal attenuation of the energy caused due to the energy dissipation by deformation in a medium. From various studies conducted on vibration decay through the soils, Bornitz[32] considered both geometric and material damping and then proposed a wave decay model. In his study, the vibrations generated by the drilled shafts were examined. These vibrations propagate through the soil as the point source rather than the line source. The Bornitz model can determine the attenuation of train-induced ground vibrations. Therefore, Equation (3) is the general form of the Bornitz equation[27, 32,33], which provides the cumulative impacts of geometric and material damping.

$$A_r = A_0 \times e^{-\alpha(r-r0)}\left(\frac{r}{r_0}\right)^n \quad (3)$$

Where A_r is the amplitude of the wave at a distance of r from the source, A_0 is the amplitude of the wave at a distance of r_0 from the source, α is the vibration decay coefficient of the material,

and n is the geometric damping coefficient. The amount of dampening caused by material damping is influenced by the soil type and vibration frequency (f). Therefore, the coefficient of material attenuation (α m^{-1}) is represented by Equation (4)[32].

$$\alpha = \frac{\pi \eta f}{V} \quad (4)$$

Where η is the damping loss factor of the soil, f is the wave frequency, and V is the wave propagation velocity. A generalized consideration of the physics of seismic wave transmission within the subsurface yields Equation (5) for predicting the α values.

$$\alpha = \frac{2\pi \xi f}{V_r} \quad (5)$$

Where ξ is the damping is the damping ratio of the material, and V_r is the Rayleigh wave velocity. The value of α depends on the material type. The stiffer soils have low values of α. In contrast, softer soils have higher values of α, as indicated from Equation (5), that α is directly proportional to the frequency of the vibration and the damping ratio of the soil. However, it is inversely proportional to the Rayleigh wave velocity. Various researchers have presented the values of α for various soil types[23, 28, 34-36]. However, very few studies have been conducted on the vibration attenuation through rocks, as various rocks' attenuation mechanisms are not well understood[37]. Table 3 presents the values of the material attenuation coefficient (α) for seismic waves having a frequency of 50 Hz.

In Equations (4) and (5), the velocity V is the Rayleigh wave velocity, i.e., V_r, because the Bornitz equation considers only the surface waves, which is the only disadvantage of this method. In the case of vibrations generated by the underground metro train, both the body (interior) waves and the surface waves are generated. Therefore, the effect of the shear wave velocity V_s and the pressure

wave velocity V_p of the wave propagation is to be considered. V_r is slightly less in value than V_s[29] and Equation (6) gives the relationship between V_r and V_s.

$$V_s = \mu V_r \quad (6)$$

where, μ is a function of poisons ratio[23].

Methodology and Research Significance

The first step in selecting a metro corridor for the study is determining where the potential for impact from GBV is the highest. The general assessment approach was employed to evaluate vibration levels at the source. The predicted values were compared to the impact criteria for general vibration evaluation to establish whether vibration influence is probable[38-41]. The purpose is to establish a relatively accurate tabulate of the people and structures that will be subjected to GBV levels that exceed the threshold. Borehole data at the particular site was recorded employing the seismic cross-hole test. The soil type was explored, and consequently, the vibration transmission along the path was assessed. Then, the dampening of vibration due to geometric and volumetric decay through the stratum was measured. Therefore, the demand for vibration mitigation has been anticipated at each chainage, and consequently, vibration control mechanisms have been proposed. With the increase in the speed of the train, the vibration along the corridor also increases; hence advanced mitigation measures are needed to control it. The current study provides insight into the vibration dampening ability of the ground with hard rock, which directly influences the design of a mitigation measure. This research will provide guidance and is relevant to track designers/researchers for accurate vibration assessment along the propagation path and the type of mitigation measure, i.e., MSS, to be adopted at varying speeds. Researchers will be able to understand in detail the considerations to be made for the future and improving the operation of the metro system.

This study considered two case studies. The first is due to the train's low speed of 80 km/h, the operational speed on the Pune Metro and most of the Indian metro corridors. The second case is for higher speeds of 250 and 350 km/h. The following codes were used to evaluate the current study: Federal Transit Administration (FTA, 2018), Research Design and Standards Organization (RDSO, 2015), ISO-2631-Part-1, 1997, and ISO-2631-Part-2, 2003[38-41].

Field Measurements

A seismic cross-hole test was conducted as per IS 13372-Part 2 (2001) to determine the attenuation of the vibration amplitude due to the geometric and material damping of seismic waves. Soil properties were determined up to 30 m at the civil court in Godown, Pune Metro, India. The geographic positions of the seismic cross-hole measurement locations are depicted in Figure 1. The equipment consisted of the freedom data PC, the PS-V electromechanical borehole source (used to generate the compression and shear waves), two numbers of triaxial geophones, and other accessories. The triaxial geophones were used to receive the seismic waves. The Olson instruments freedom data PC with the cross-hole seismic system and Wingeo software was used to record the P-SV source input and the receiver outputs. It was found that the soil stratum was homogeneous basalt rock. Different parameters such as insitu shear and compression wave velocity, dynamic poison's ratio, Young's modulus, and shear modulus were determined and are presented in Table 4.

The test was conducted by generating compression and shear waves traveling horizontally at a particular depth in one borehole, i.e., the source borehole. Their arrival was recorded at the same depth in two nearby boreholes, i.e., receiving boreholes, as shown in Figure 2. After recording the travel times and travel distance at each measurement depth, wave velocities were calculated.

Five boreholes in two mutually perpendicular directions, spaced about 4 m apart at every location, were drilled using the rotary drilling technique for cross-hole seismic testing. Of these boreholes, the corner borehole (BH 03), which is at a distance of 3 m and 6 m from the receiver boreholes 2 and 1, respectively, was considered the source borehole for generating seismic waves. The remaining four boreholes were used for lowering triaxial geophones at various depths to record P and S wave arrivals. The logging interval was maintained at 1.5 m by moving the source and recording the geophone in the respective boreholes step by step. The test started from the bottom of the borehole and was conducted up to 1 m depth. Each test at a particular depth was repeated thrice in the up and down directions to ensure consistency in the velocities measured. The average of the three sets of velocities at each depth was considered the expected value for a particular depth.

Data Processing

The collected data were processed using the WINGEO analysis program by Olson Instruments, Inc. From the seven channels taken in the study, at channels 1, 2, and 3, the first triaxial geophone was used; at channels 4, 5, and 6, the second triaxial geophone had been used; and at channel 7, the cross-hole source trigger had been used.

The arrival of the shear wave energy is often indicated by a split in the wave's polarization, as shown in Figure 3. The down-impact direction is recorded in magenta, and the corresponding shear wave energy will show a positive break. The opposite is true for the up-impact direction. The corresponding shear wave energy in the up-direction will show a negative break.

The arrival of the compression wave energy is indicated by the first break, positive or negative, at a given depth after the trigger offset has been accounted for (Figure 4).

As outlined above, the down-hole source arrival time is corrected to zero by selecting the breaking point for each depth. Once the break time is selected, and the zero function is enabled, both the up and down components should line up on zero, as shown in Figure 5. Figure 6 shows the compression and shear seismic velocities obtained from the study.

Results and Discussions

According to RDSO, FTA and ISO-2631, Part 1 guidelines, a vibration level of less than 0.1 mm/s or 72 VdB is acceptable for human comfort at a reference speed of 2.54×10^{-5} mm/s. On the other hand, vibration levels greater than 72 VdB are uncomfortable for humans. That indicates the maximum allowable vibration limit at the ground considering the human response to vibrations 72 VdB[38-40]. However, according to ISO-2631, Part 2 standards, if the value of vibration exceeds 100 VdB, a crack will develop in the structure[41]. Therefore, it is necessary to know the vibration at the source, how much it gets damped along the path, and finally, which vibration attenuation system should be adopted at the source. This study uses Equation (2) to calculate the geometric damping and Equation (3) to calculate the material damping. For calculating geometric damping, the value of S has been taken as 10 VdB as per Table 1, and the value of α has been taken as 0.414 km^{-1} as per Table 3. Table 5 provides the total amount of vibration decay along the propagation path.

Case- I: For a train speed of 80 km/h

In this study, the chainages 11320– 1680, 12000–12300, 12700–12800, 13400–13960, 13960–14500, 14520–15180, and 15180–16400 of the Pune Metro line (North-South corridor) were taken into account. The maximum design speed of the train is 90 km/h, but the maximum operating speed is 80 km/h. The axle load of the train has been considered as 16 tonnes, and the unsprung mass of 15% has been considered. The maximum vibration of 92 VdB (global value) is considered

the train emission from a 16-ton train with an operating speed of 80 km/h, as per the guidelines[38, 39].

According to the RDSO and FTA guidelines, vibration levels must be added to or subtracted based on factors such as track structure conditions, the number of building stories, and more. As a result, in the current study, a +5 VdB correction for the jointed track structure was used because the slab tracks are connected using dowel joints. Now, if the factors such as corrugation, general wear, or mill scale occur on a new track, then the adjustments in vibration levels are to be taken as +5 to +15 VdB higher than the expected value. Here, the minimum increase was considered, i.e., +5 VdB.

Vibration levels are often attenuated as they are transmitted through the building. In response, resonances in the structural system, especially the floors, will generate considerable vibration amplification. Modifications for the first floor, considering a basement, are as follows: For coupling loss, -5 VdB; for the propagation of vibration energy from the basement to the first floor, an adjustment of -2 VdB; and a +6 VdB adjustment for the floor amplification are adopted[38, 39]. Therefore, here the total adjustment, is -5-2+6 = -1 VdB.

A total vibration of 92+5+5-1 = 101 VdB will be observed at the source, considering the above modifications in vibration levels. The majority of the modifications are highly influenced by the excitation force frequency range and vibration transmission frequency dependence. It is vital to highlight that if the form of the exact vibration spectrum is not adequately examined, an improper vibration control technique may be selected, increasing vibration levels.

From Table 4, the average shear wave velocity of 2900 m/s has been taken in the study. As the shear velocity along the propagation path is very high, vibration decay is mainly due to the volumetric decay and not the soil/material damping decay, as shown in Table 5. The average path

decay of vibration has been considered, i.e., 10 VdB. Therefore, the vibration reaching the structures is 101-10 = 91 VdB. So, there is a need to attenuate 91-72 = 19 VdB of vibration for human and structural comfort. It is to be noted that vibration on the ground floor will be 91 VdB during a single train pass-by condition, and it will be approximately 94 VdB when the two trains cross simultaneously[38, 39].

Case- II: For higher train speeds of 250 and 350 km/h

GBV levels fluctuate around 20 times the logarithm of the speed. That means doubling the train speed increases the vibration responses by about 6 VdB. Therefore, for a speed of 180 km/h, the magnitude of the vibration will be doubled for an increase of every 6 VdB, and for a speed of 350 km/h, the magnitude of the vibration will be almost four times as high at the source. Equation (7) is the generalized formula used to calculate the vibration emission levels at other train speeds, in which the reference speed is taken as 80 km/h[38, 39, 41]. So, for a maximum operating speed of 250 km/h and 350 km/h, the vibration levels of 101 VdB and 104 VdB are predicted to be generated at the source.

$$VdB = 20log\frac{V}{V_{Ref.}} \quad 7$$

After all the adjustments, same as in case-I, are applied to the vibration levels generated by a speed of 250 km/h, a total vibration emission of 101+5+5-1 = 110 VdB will be observed at the source. Taking the path decay of vibration as an average of 10 VdB from Table 5, the vibration reaching the structures will be 110-10 = 100 VdB. So, there is a need to attenuate 112-72 = 28 VdB of vibration for a speed of 250 km/h. Similarly, for a speed of 350 km/h, the vibration reaching the structures will be 103 VdB, so the amount of vibration to be attenuated is 103-72 = 31 VdB.

Proposition of mass-spring systems

The vibration-attenuating ability of the rock strata is found to be low due to their higher shear wave velocity (Table 5). Therefore, depending on the vibration decay results along the propagation path, Table 6 presents the recommendation of MSS for the vibration emission at 80, 250, and 350 km/h, respectively. At the curve portion, vibration adjustment of +5 VdB is applied due to the high dynamic interaction between the rail and wheel. To obtain a better design, ± 3 VdB can be adjusted[38, 39, 42].

For a speed of 80 km/h, the mitigation measure, i.e., discrete P-MSS with a natural frequency of 13–14 Hz and S-MSS with a natural frequency of 7–8 Hz, has been suggested to attenuate the vibration of about 15–17 VdB and 20–23 VdB, respectively. Only S-MSS has been suggested for the higher speeds due to the high vibration emissions. Therefore, for a speed of 250 km/h, a mitigation measure with a natural frequency of 6–7 Hz and 4.5–5 Hz has been suggested to attenuate 23–28 VdB and 31–34 VdB of vibration, respectively. Similarly, for a speed of 350 km/h, mitigation measures with a natural frequency of 4–5 Hz, 5 Hz, and 6–7 Hz should be adopted to attenuate 31–36 VdB, 31 VdB, and 23–28 VdB of vibration, respectively.

Conclusion

The characteristics of propagation and absorption of vibrations within the basaltic rock strata caused by train loading were examined, and the following inferences were drawn for the study:

- With increasing ground depth, the geometric decay of vibration energy increases, and an average of 10 VdB has been deducted from the source vibration. However, no vibration decay, i.e., 0 VdB, was observed due to material dampening.

- The vibration attenuation requirement of the system increases in direct proportion to the train's speed. Therefore, low-frequency mitigation techniques were proposed to reduce the high-magnitude vibrations.
- Two MSS, i.e., discrete P-MSS and S-MSS, have been proposed depending on the source's vibration emissions. For vibration emissions of less than 18 VdB, P-MSS and vibrations above 18 VdB, S-MSS are more suitable.
- The vibration intensity increases by nearly +5 VdB along the curve of the track structure system due to the significant dynamic interaction between the rail and wheel. As a result, at the curves, S-MSS is observed to be more acceptable.

Declaration of conflicting interests

The authors declare no potential conflicts of interest concerning this article's research, authorship, and publication.

Acknowledgment

The authors wish to thank the Director, CSIR- Central Road Research Institute, New Delhi, and the Academy of Scientific and Innovative Research, Ghaziabad, for permitting us to publish this paper. The authors also thank the CSIR-Human Resource Development Group for awarding a Senior Research Fellowship to Ms. Shamsul Bashir for conducting this research.

References

1. Miller, G. F., Pursey, H. and Bullard, E. C., On the partition of energy between elastic waves in a semi-infinite solid. Proceedings of the Royal Society A, 1955, Vol. 233, Issue 1192, pp. 55–69, https://doi.org/10.1098/rspa.1955.0245.
2. Kouroussisa, G., Connolly, D. P. and Verlinden, O., Railway-induced ground vibrations – a review of vehicle effects. International Journal of Rail Transportation, 2014, Vol. 2, Issue 2, pp. 69-110, https://doi.org/10.1080/23248378.2014.897791.
3. Yang, Y. B. and Hsu, H. L., A Review of Researches on Ground-Borne Vibrations Due to Moving Trains via Underground Tunnels. Advances in Structural Engineering, 2006, Vol. 9, Issue 3, pp. 377-392, https://doi.org/10.1260/136943306777641887.
4. Railway Induced Vibration, State of the Art Report. International Union of Railways (UIC), 2017, pp. 1-82.
5. Eitzenberg, A. Train Induced Vibrations in Tunnels: A Review. Lulea University of Technology. Lulea, Sweden, 2008, pp. 1-90.
6. Connolly, D. P., Kouroussis, G., Woodward, P. K., Costa, P. A., Verlinden, O. and Forde M. C., Field testing and analysis of high-speed rail vibrations. Soil Dynamics and Earthquake Engineering. 67:102-118, https://doi.org/10.1016/j.soildyn.2014.08.013.
7. Ribes-Llario, F., Marzal, S., Zamorano, C. and Real, J., Numerical Modelling of Building Vibrations due to Railway Traffic: Analysis of the Mitigation capacity of a Wave Barrier. Hindawi, Shock and Vibration, 2017, Article ID 4813274, pp. 1-11, https://doi.org/10.1155/2017/4813274.

8. Remington, P. J., Kurzweil, L. G., and Towers, D. A. Low Frequency Noise and Vibrations from Trains. Transportation Noise Reference Book, Nelson PM. London: Boston: Butterworth, 1987.
9. Yang, Y. B., Hung, H. H., Hsu, L. C. Ground vibrations due to underground trains considering soil-tunnel interaction. Interaction and Multiscale Mechanics, 2007, Vol. 1, Issue 1, pp. 157-175, https://doi.org/10.12989/imm.2008.1.1.157.
10. Shi, W., Miao, L., Luo, J. and Zhang, H. The Influence of the Track Parameters on Vibration Characteristics of Subway Tunnel. Hindawi, Shock and Vibration, 2018, Article ID 2506909, pp. 1-12, https://doi.org/10.1155/2018/2506909.
11. Yang, Y. B. and Hung, H. H. Soil Vibrations Caused by Underground Moving Trains. Journal of Geotechnical and Geoenvironmental Engineering, 2008, Vol. 134, Issue 11, pp. 1633-1644, https://doi.org/10.1061/ (ASCE) 1090-0241.
12. Wang, W., Liu, W., Sun, N. and Ma, M. Study on Vibration Bounce Area Caused by Metro-Based on the Pulse Impact Experiment. 2nd International Conference on Electronic & Mechanical Engineering and Information Technology. Advances in Intelligent Systems Research., 2012, pp. 0839-0843. https://doi.org/10.2991/emeit.2012.18.
13. Eitzenberger, A. Inventory of geomechanical phenomena related to train-induced vibrations from tunnels. Luleå University of Technology Department of Civil, Mining and Environmental Engineering Division of Mining and Geotechnical Engineering, 2008:54, ISSN: 402-1757, ISRN: LTU-LTC, 08⁄54, SE, pp. 1-84.
14. Kouroussis, G., Parys, L. V., Conti, C. and Verlinden, O. Prediction of ground vibrations induced by urban railway traffic: an analysis of the coupling assumptions between vehicle,

track, soil and building. International Journal of Acoustics and Vibration, 2013, Vol. 18, Issue 4, pp. 163–172, 10.20855/ijav.2013.18.4330.

15. Shi, W., Bai, L. and Han, J. Subway-Induced Vibration Measurement and Evaluation of the Structure on a Construction Site at Curved Section of Metro Line. Hindawi, Shock and Vibration, Article ID 5763101, 2018, pp. 1-18, https://doi.org/10.1155/2018/5763101.
16. Zou, C., Wang, Y. and Tao, Z. Train-Induced Building Vibration and Radiated Noise by Considering Soil Properties. Sustainability, 2020, pp. 1-17, https://doi:10.3390/su12030937.
17. Vogiatzis, K. and Mouzakis, H. Ground-Borne Noise and Vibration Transmitted from Subway Networks to Multi-Storey Reinforced Concrete Buildings. Transport, 2018, Vol. 33, Issue 2, pp. 446-453, https://doi.org/10.3846/16484142.2017.1347895.
18. Yao, J. and Fang, L. Building Vibration Prediction Induced by Moving Train with Random Forest., Hindawi, Journal of Advanced Transportation, Article ID 6642071, 2021, pp. 1-13, https://doi.org/10.1155/2021/6642071.
19. Hu, J., Bian, X. and Jiang, J. Critical Velocity of High-Speed Train Running on Soft Soil and Induced Dynamic Soil Response. Procedia Engineering. Advances in Transportation Geotechnics 3. The 3rd International Conference on Transportation Geotechnics, 2016, Vol. 143, pp. 1034–1042, Doi: 10.1016/j.proeng.2016.06.102.
20. Krylov, V. V. Ground Vibrations from High-Speed Railways Prediction and mitigation. ICE Publishing, London, 2019, ISBN: 978-0-7277-6379-2.
21. Krylov, V. V. Ground Vibration Boom from High-Speed Trains. Journal of Low Frequency Noise, Vibration and Active Control, 1999, Vo. 18, Issue 4, pp. 207-218.
22. Krylov, V. V. Noise and vibration from high-speed trains. London: Thomas Telford, 2001.

23. Richart, F. E., Hall, J. R. and Woods, R. D. Vibrations of Soils and Foundations. Prentice-Hall Inc., Eaglewood Cliffs, New Jersey, 1970, pp. 1-216.
24. Ewing, W. M. and Jardetzky, W. S. Elastic Waves in Layered Media. McGraw-Hill Book Co., New York, 1957.
25. Attewell, P. B. and Farmer, I. W. Attenuation of Ground Vibrations from Pile Driving. Ground Engineering, 1973, Vol. 6, Issue 4, pp. 26-29. http://worldcat.org/issn/00174653.
26. Gotowski, T. G. and Dym, C. L. Propagation of Ground Vibration: A Review. Journal of Sound and Vibration. 1976, Vol. 49, Issue 2, pp. 79-93, https://doi.org/10.1016/0022-460X (76)90495-8.
27. Das, B. M. Fundamentals of soil dynamics. Elsevier Science Publishing Co., New York, 1983, pp. 1-399.
28. Woods, R. D. Screening of Surface Waves in Soils. Journal of the Soil Mechanics and Foundations Division, ASCE, 1968, Vol. 94, pp. 951-979.
29. Athanasopoulos, G. A., Pelekis, P. C. and Anagnostopoulos, G. A. Effect of soil stiffness in the attenuation of Rayleigh-wave motions from field measurements. Soil Dynamics and Earthquake Engineering, 2000, Vol. 19, Issue 4, pp. 277–288, https://doi.org/10.1016/S0267-7261 (00)00009-9.
30. Kim, D. S. and Lee, J. S. Propagation and attenuation characteristics of various ground vibrations. Soil Dynamics and Earthquake Engineering, 2000, Vol. 19, Issue 2, pp. 115-126, https://doi.org/10.1016/S0267-7261 (00)00002-6.
31. Amick, H. and Gendreau, M. Construction vibrations and their impact on vibration-sensitive facilities. Construction Congress VI, ASCE Library, 2000, https://doi.org/10.1061/40475 (278)80.

32. Bornitz, G. Über die Ausbreitung der von Grobkolbenmaschinen erzeugten Bodenschwingungen in die Tiefe (About the propagation of the ground vibrations generated by large piston machines into the depths), Springer, Berlin, 1931.
33. Mintrop, L. Uber die Ausbreitung der von den Massendrucken einer Grossasmaschine erzeugten Bodenschwingungen (About the spread of the ground vibrations generated by the mass pressures of a large gas engine). Ph.D. Dissertation, University of Gottingen, Gottingen, Germany, 1911.
34. Kushida, H. Engineering of Environmental Vibration, Rikodosho, Tokyo, 1997.
35. Peng, S. M. Propagation and Screening of Rayleigh Waves in Clay. Master's Engineering Thesis, Asian Institute of Technology, Bangkok, 1972.
36. Barkan, D. D. Dynamics of Bases and Foundations. McGraw Hill Book Company, 1962.
37. Dobrin, M. B. and Savit, C. H. Introduction to Geophysical Prospecting. Fourth Edition, McGraw-Hill Book Company, 1988, pp. 39-48.
38. Federal Transit Administration-FTA, Transit Noise and Vibration Impact Assessment Manual. FTA Report No. 0123, National Transportation Systems Center, 2018.
39. Metro Rail Transit System, Guidelines for Noise and Vibrations. CT- 38, Track Design Directorate, Research Designs and Standards Organisation (RDSO)-ISO-9001, Ministry of Railways, India, 2015.
40. ISO-2631-Part-1 Mechanical Vibration and Shock-Evaluation of human exposure to whole-body vibration-Part 1: General Requirements, 1997.
41. ISO-2631-Part-2 Mechanical vibration and shock — Evaluation of human exposure to whole-body vibration-Part 2: Vibration in buildings (1 Hz to 80 Hz), 2003.

Table 1. Geometric attenuation coefficient (n)[26, 30].

S.No.	Physical Source	Type of Source	Location of source	Type of wave	n	S
1	Highway/Rail line/ footing/Array	Line	Surface	Surface	0	0
			Surface	Body	1	20
2	Car into pothole/ Single footing	Point	Surface	Surface	0.5	10
			Surface	Body	2	40
3	Tunnel	Buried line	Interior	Body	0.5	10
4	Buried explosion	Buried point	Interior	Body	1	20

Table 2. Geometric attenuation coefficient[31].

Sl.No.	Position	Type of wave	Observation point	n
1	Point source on surface	Rayleigh	Surface	0.5
2	Point source on surface	Body	Surface	2
3	Point source at depth	Body	Surface	1
4	Point source at depth	Body	At depth	1

Table 3. Value of α at 50 Hz[37]

Material and Source	Velocity (km/s)	α (km^{-1})
1. Granite		
Quincy, Mass	5	0.2-0.3
Rockport, Maine	5.1	0.237
Westerly, RI	5	0.384
2. Basalt		
Painesdale, Mich	5.5	0.414
3. Diorite	5.78	0.21

Table 4. Dynamic properties of soil

Compression wave velocity, V_s (m/s)	**Shear wave Velocity, V_r (m/s)**	**Young's Modulus, E (kPa)**	**Shear Modulus, G (kPa)**	**Poisons Ratio, υ**
3812 - 5333	2170 - 2909	2.90×10^7 - 5.24×10^7	1.14×10^7 - 2.03×10^7	0.22 – 0.30

Table 5. Vibration decay data along the propagation path

Depth (m)	Shear Velocity (m/s)	Frequency (Hz)	Volumetric Decay (VdB)	Soil/Material Decay (VdB) for $\alpha = 0.414\ km^{-1}$	Total Decay (VdB)
15	2900	50-60	7	0	7
17			8	0	8
19			8	0	8
21			8	0	8
23			9	0	9
25			9	0	9
27			10	0	10
29			10	0	10
31			10	0	10
33			10	0	10
35			11	0	11
37			11	0	11

Table 6. Recommendations for MSS at different train speeds

Chainage (m)	Section	Rail level depth (m)	80 km/h			250 km/h			350 km/h			
			Vibration at GL (VdB)	MSS frequency (Hz)	Mitigation (VdB)	Vibration at GL (VdB)	MSS[1] frequency (Hz)	Mitigation (VdB)	Vibration at GL (VdB)	MSS[1] frequency (Hz)	Mitigation (VdB)	Permissible limit (VdB)
11320-11680	Straight	15-17	91	13-14 (P*)	15-17	100	6-7	23-28	103	5	31	72
12000-12300	Curve	23-25	91+5 =96	7-8 (S**)	20-23	100+5 =105	4.5-5	31-34	103+5 =108	4-5	31-36	72
12700-12800	Minor curve	27-29	91	13-14 (P*)	15-17	100	6-7	23-28	103	6-7	23-28	75[2]
13400-13960	Curve	21-24	91+5 =96	7-8 (S**)	20-23	100+5 =105	4.5-5	31-34	103+5 =108	4-5	31-36	72
13960-14500	Straight	21-26	91	13-14 (P*)	15-17	100	6-7	23-28	103	5	31	72
14520-15180	Curve	17-21	91+5 =96	7-8 (S**)	20-23	100+5 =105	4.5-5	31-34	103+5 =108	4-5	31-36	72
15180-16400	Straight	19-23	91	13-14 (P*)	15-17	100	6-7	23-28	103	5	31	72

Note: *S-MSS, **P-MSS, [1]MSS's suggested for 250 and 350 km/h are S-MSS's, and [2]75 VdB is the vibration limit for day time

Figure 1. Map of site showing the location of boreholes

Figure 2. Seismic cross borehole test set-up

Figure 3. Shear wave arrival showing split in polarized energy

Figure 4. Compression wave arrival picking

Figure 5. Trigger Zeroing

Figure 6. Variation of seismic velocity with depth

Figure 1. Map of site showing the location of boreholes

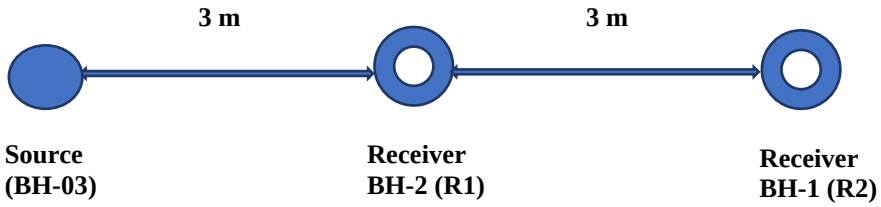

Figure 2. Seismic cross borehole test set-up

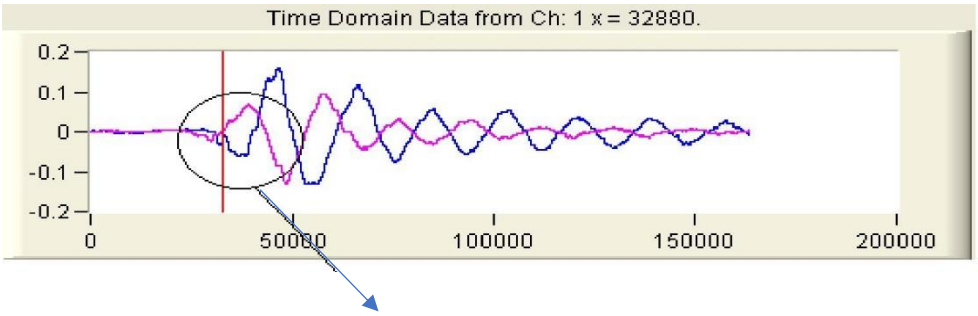

Shear wave arrival showing split in polarized energy

Figure 3. Shear wave arrival showing split in polarized energy

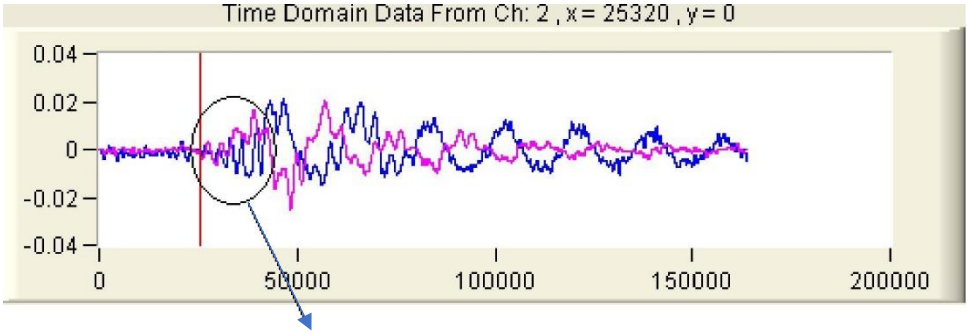

Figure 4. Compression wave arrival picking

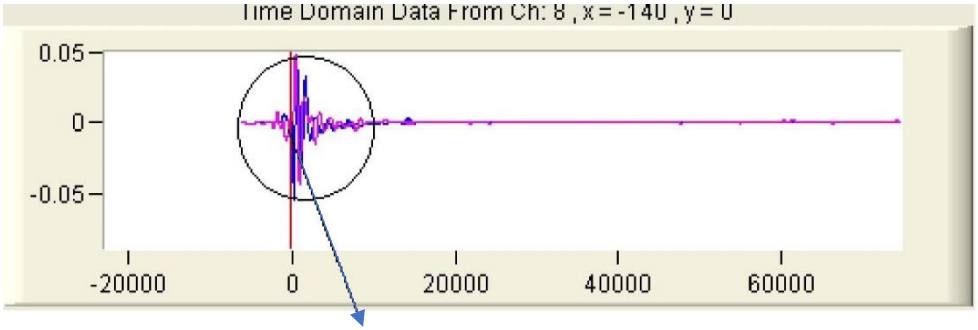

Figure 5. Trigger Zeroing

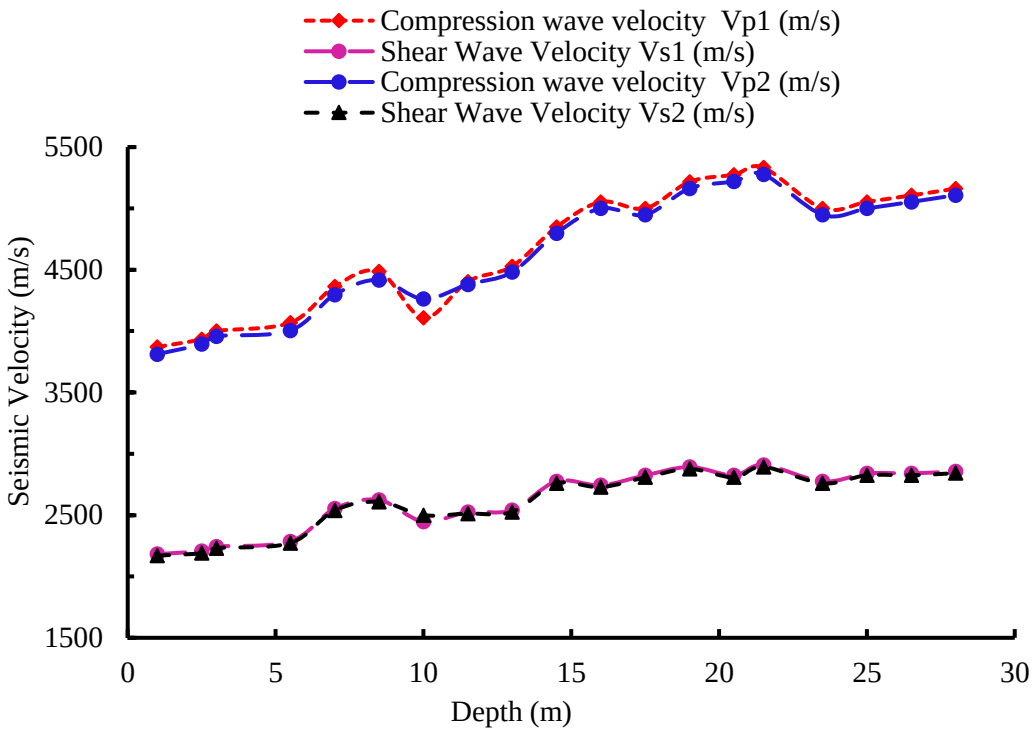

Figure 6. Variation of seismic velocity with depth